ELSEVIER

Microelectronic Engineering 66 (2003) 281–288

MICROELECTRONIC ENGINEERING

www.elsevier.com/locate/mee

Influence of contamination on the electrical activity of crystal defects in silicon

Martin Kittler*, Winfried Seifert, Klaus Knobloch

IHP—Innovations for High Performance Microelectronics, Im Technologiepark 25, 15236 Frankfurt (Oder), Germany

Abstract

It is shown by EBIC that dislocation activity is controlled by the degree of metal contamination. The activity can be affected by external gettering and hydrogenation. DLTS investigations showed that the occurrence and features of the dislocation-related C1 line also depend on the amount of contamination. In small amounts, the impurities are believed to be tightly bonded to the dislocation core, resulting in a rather sharp energetic distribution of levels of the C1 line. At larger concentrations, the impurities are accommodated as a cloud in the dislocation strain field, giving rise to a broad energetic distribution of levels of C1. It is suggested that only impurity atoms in the cloud can be removed by external gettering and/or passivated by hydrogenation.

Keywords: Dislocations; Electrical activity; Silicon; Gettering; Passivation

1. Introduction

Extended crystal defects in Si, such as dislocations or precipitates, may have a detrimental influence on device performance due to their electrical activity. Thus, the generation of process-induced defects in the active device region has to be avoided. On the other hand, during microelectronics processing, crystal defects are often formed intentionally as preferential gettering sites far away from the device, with the purpose of attracting metal impurities and keep them in the wafer interior (internal gettering). However, electrically active defects in the wafer bulk cause a diffusion current that may enhance the leakage of reverse-biased devices at elevated temperatures (see, e.g., Refs. [1,2]). This disturbing electrical action of the defects/gettering sites in the wafer interior was found to increase with their gettering action (see, e.g., Ref. [3]). Accordingly, understanding the influence of impurities on the electrical activity of crystal defects is still of interest for microelectronics. Recently, increased attention to the issue of defect activity was triggered by Si photovoltaics. The use of low-cost

*Corresponding author. Tel.: +49-335-5625-130; fax: +49-335-5625-327.
E-mail address: kittler@ihp-microelectronics.com (M. Kittler).

0167-9317/02/$ – see front matter
doi:10.1016/S0167-9317(02)00919-X

multicrystalline Si for solar cells demands alternative strategies for defect engineering since crystal defects/dislocations are inherent in this material. Improved knowledge of the interaction between impurities and extended defects is essential for further progress in this area.

In this paper we discuss the characterization techniques and findings related to the electrical activity of dislocations. After a brief review of our results obtained by using the technique of electron-beam-induced current (EBIC), we give a detailed report on deep-level transient spectroscopy (DLTS) investigations. It is shown that the DLTS results allow a deeper insight into the accommodation of impurities at/near dislocations and a better understanding of the limits of gettering and hydrogenation treatments.

2. EBIC

The recombination properties of extended crystal defects in Si are mainly defined by recombination-active impurities decorating the particular defects, i.e. the recombination activity is not an intrinsic defect property, but of extrinsic origin. Even chemical-mechanical polishing [4] may cause defect contamination and increase defect activity. Temperature-dependent EBIC investigations of the recombination activity of dislocations clearly demonstrates the role of defect contamination (see, e.g., Ref. [5]). Both the magnitude of the contrast and its temperature dependence $c(T)$ have been found to depend on the amount of contamination (see Fig. 1). The $c(T)$ behaviour represents a fingerprint characterizing the degree of contamination of the crystal defects. Clean dislocations exhibit only very weak activity (type II), with a maximum at about 50 K and untraceable activity at room temperature. Weak contamination leads to an increase of the low temperature activity, still leaving the room temperature activity below the detection limit (type 2). Upon a further increase in contamination the type of temperature dependence changes and defect activity is also detected at room temperature (type 1). A similar influence of contamination was observed for defects formed by oxygen precipitation in

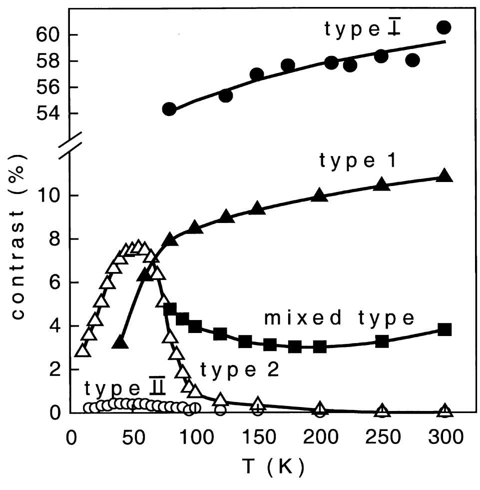

Fig. 1. Temperature dependence of the EBIC contrast of dislocations, $c(T)$, for different concentrations of contaminating impurities. Change of contrast type with increasing contamination is in the sequence: type II (clean)→type 2→mixed→type 1→type I.

CZ-Si [6]. Finally, dislocations decorated with metal silicide precipitates have the highest activity throughout the whole temperature range (type I). Internal Schottky junctions at the metal silicide particles that attract minority carriers and facilitate fast recombination are the cause of the strong activity (e.g., Ref. [7]).

Experiments with hydrogenation and phosphorus diffusion gettering have shown that both the passivation and gettering of impurities decorating dislocations change the $c(T)$ behaviour in the reverse sequence, from type 1 to type 2. However, the very small intrinsic activity (type II behaviour) cannot be restored. The type 2 behaviour has been found to represent the lower limit of activity that may be achieved by gettering and hydrogenation [8,9], corresponding to about 10^4–10^5 deep levels/impurities per cm dislocation length (see below).

A model describing the dislocation $c(T)$ behaviour gives quantitative access to the concentration of the deep-level impurities at dislocations [10]. It gives the following numbers of impurities per unit length for the types of behaviour denoted in Fig. 1: type II (clean), no impurities; type 2, about 10^4–10^5 impurities per cm dislocation length; type 1, 10^6 impurities per cm or more (for the mixed-type behaviour the number of impurities is between those for types 1 and 2). The model assumes that shallow one-dimensional dislocation bands (about 80 meV from the band edges), induced by the dislocation strain field, and deep electronic levels, caused by impurity atoms segregated at the dislocations, can exchange electrons and holes. This is because the wave functions of impurity atoms—which are spatially located at or near the dislocation core at a distance not exceeding a few nm—and the one-dimensional dislocation bands overlap. As a consequence, the recombination of carriers captured at the one-dimensional dislocation bands can be drastically enhanced by the presence of even small concentrations of impurity atoms at the dislocation.

3. DLTS

Using DLTS we analyzed misfit dislocations in Si–SiGe (2%) stacks of n-type conductivity which were used as a kind of ''model defect''. The 60° misfit dislocations were located at a depth of about 2.3 μm below the surface. Samples with initially clean dislocations were contaminated with different amounts of gold, giving rise to either type 2 or mixed type/type 1 EBIC $c(T)$ behaviour. In samples with clean dislocations (type-II behaviour) DLTS revealed one peak of an electron trap, MF.E1. In the intentionally contaminated samples with dislocations of type-2 or mixed type/type-1 behaviour, we observed three electron traps, MF.E1, MF.E2 and MF.E3 (see Fig. 2). We have clear evidence that only MF.E3 is due to the misfit dislocations (for details, see Ref. [11]). Arrhenius plots of the dislocation-related trap MF.E3—giving an apparent enthalpy in the range between 0.39 and 0.52 eV—were found to be very similar to the plots of the C1 line as observed by Omling et al. [12] and Cavalcoli et al. [13], for example. Accordingly, we believe that the electron trap MF.E3 is identical to the well-known C1 line.

Note that the C line is the most prominent dislocation-related line (in n-Si). It should be pointed out that this line could only be observed for contaminated dislocations. Clean dislocations did not show this line (see also Ref. [14]).

Compared with the DLTS peak of point defects the C line is considerably broadened. On variation of the duration of the filling pulse, t_p, different behaviour of the C line is reported in the literature. The line shape was observed to be either symmetrically or asymmetrically broadened (e.g., Refs. [13,15]).

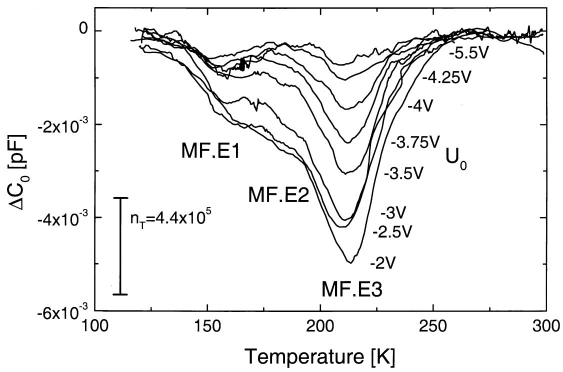

Fig. 2. DLTS spectra recorded with varying filling pulse height U_0 at pulse length $t_p = 1$ ms, reverse bias $U_R = -8$ V, and emission rate $\tau^{-1} = 100\ s^{-1}$. The axis ΔC_0 describes the absolute change of the capacitance, which is directly proportional to the number of states. Contaminated dislocations exhibiting type 2 behaviour contain three electron traps, MF.E1, MF.E2 and MF.E3. Only MF.E3 is due to the dislocations.

We found that these differences are related to the degree of contamination. We observed that differing amounts of contamination of the dislocations (with type 2 or mixed type/type 1 behaviour) affects the t_p dependence of the C1 line and the energetic distribution of the dislocation-related states. To determine whether the distribution is sharp or broad we used a mode of measurement that benefits from the well-defined depth location of the misfit dislocations in our samples (at the interface between the Si cap and the SiGe layer): the height of the filling pulse, U_0, was kept constant while spectra were recorded at different values of the reverse bias, U_R, applied during the emission cycle of electrons from the dislocation-related states. The larger the bias U_R the greater is the band bending, i.e. the deeper states can take part in the process of emission of electrons. Consequently, if there is a broad distribution of states we would expect that the maximum of the DLTS peak would shift to higher temperatures when U_R is increased (assuming that the capture cross-section of the states is nearly constant).

3.1. Dislocations with type-2 EBIC behaviour

The C1 line was observed to remain symmetric during variation of the filling pulse t_p and the peak position was found not to shift on the temperature scale (see Fig. 3(a)). Using the special mode of measurement described above, we found that the position of the C1 line remains nearly constant when the reverse bias U_R is varied (see Fig. 3(b)). There is a very small shift of the peak from 215 K at $U_R = -8$ V to 210 K at -4 V, only. Accordingly, we conclude a rather sharp energetic distribution of the dislocation-related states.

3.2. Dislocations with mixed type/type-1 EBIC behaviour

In this sample the contamination of dislocations is stronger. We observed that the C1 line becomes more and more asymmetric upon increase of t_p, while the position of the line maximum remains constant (see Fig. 4(a)). Measurements using the special mode with variation of U_R showed a significant shift of the maximum of the DLTS peak (see Fig. 4(b)). The peak shifts from 185 K at

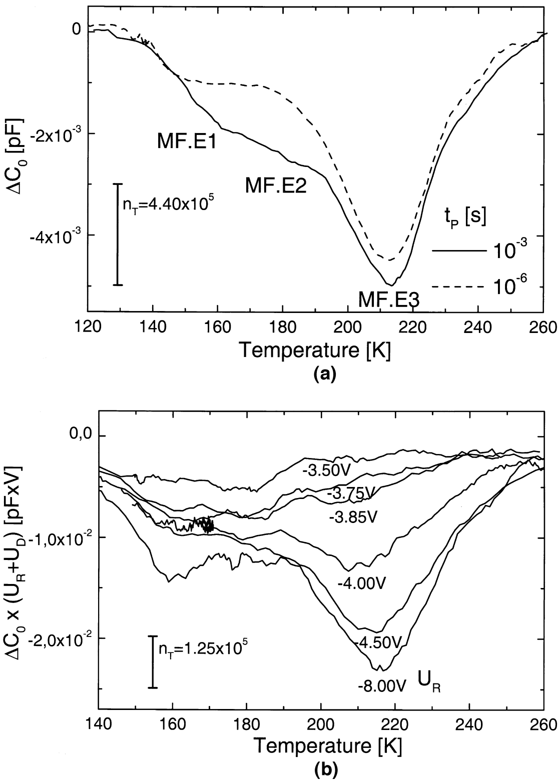

Fig. 3. DLTS spectra of dislocations exhibiting type 2 behaviour. (a) Dependence on the duration t_p of the filling pulse. Fixed parameters are the height of the filling pulse $U_0 = -2$ V, the reverse bias $U_R = -8$ V, and the emission rate $\tau^{-1} = 100$ s^{-1}. (b) Dependence on the reverse bias U_R. Fixed parameters are the height of the filling pulse $U_0 = -2$ V, the duration of the filling pulse $t_p = 1$ ms, and the emission rate $\tau^{-1} = 100$ s^{-1}. This mode of measurement benefits from the well-defined depth location of the dislocations. The scaling of the y-axis, $\Delta C_0(U_R + U_D)$, takes into account the influence of the reverse bias and of the diffusion voltage. This allows us to directly compare the absolute number of recharged levels. The measurements yield a rather sharp energetic distribution of dislocation-related levels for the C1 line.

$U_R = -3.5$ V to 212 K at $U_R = -8.0$ V. This indicates a broad energetic distribution of the dislocation-related states, with a width of about $\Delta E = 50$ meV.

3.3. Number of states

An estimate of the absolute number of states related to the C1 line, n_T, as observed by DLTS under a Schottky contact of 1 mm diameter gives for type 2 dislocations a few 10^5 states and for dislocations with mixed type/type 1 behaviour a few 10^6 states, i.e. the difference between the samples amounts to about one order of magnitude. The total dislocation length under the contact was estimated to be in the region of 10 cm for both samples. Consequently, the state density per cm dislocation length is calculated to be a few 10^4 or a few 10^5 per cm, respectively. This is in good agreement with estimates of the dislocation contamination as found by EBIC.

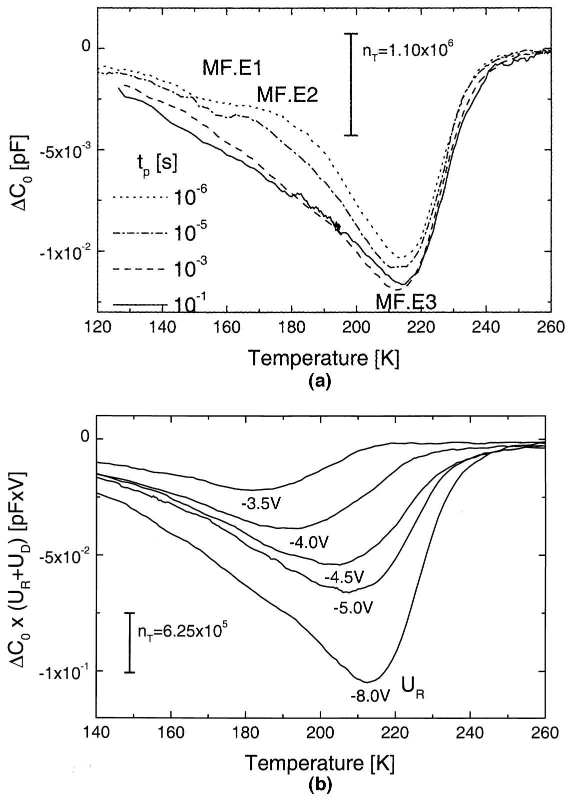

Fig. 4. DLTS spectra of dislocations exhibiting mixed type/type 1 behaviour. (a) Dependence on the duration t_p of the filling pulse. Fixed parameters are the height of the filling pulse $U_0 = -2$ V, the reverse bias $U_R = -8$ V, and the emission rate $\tau^{-1} = 100\ s^{-1}$. (b) Dependence on the reverse bias U_R. Fixed parameters are the height of the filling pulse $U_0 = -2$ V, the duration of the filling pulse $t_p = 1$ ms, and the emission rate $\tau^{-1} = 100\ s^{-1}$. The measurements yield a broad distribution of dislocation-related levels ($\Delta E = 50$ meV) for the C1 line.

4. Discussion

Using standard DLTS we observed that the position of the C1 maximum remained constant upon variation of t_p (see Figs. 3(a) and 4(a)). The fact that the position of a DLTS peak stays constant upon variation of t_p is an indication that this peak is formed by a distribution of levels and not by band-like states (see Ref. [16]). Therefore, we conclude that C1 is due to levels which are presumably caused by impurities. Indeed, the number of impurities as observed by EBIC agrees with the number of dislocation-related levels found by DLTS. According to the EBIC model [10] the impurities must be accommodated very close to the dislocations at a distance not exceeding a few nm.

The width of the energetic distribution of the levels forming the C1 line increases with the degree of contamination or number of levels. It is found to be rather sharp for dislocations with type 2 behaviour (Fig. 3(b)) and to become broad/smeared out ($\Delta E = 50$ meV) for dislocations with mixed type/type 1 behaviour (Fig. 4(b)), exhibiting a higher contamination density.

The reason for this dependence may be explained by a rather simple picture. We assume that the level and the related properties of a point defect/impurity atom are influenced by the configuration of the surrounding Si atoms. This means the point defects/impurities at dislocations are exposed to local potentials, whereby their levels will be modified as compared to isolated point defects/impurity atoms in the regular Si lattice. The surrounding point defects/impurities accommodated in the dislocation core differ strongly from the regular Si lattice. Point defects located in the cloud formed by the dislocation strain field experience surroundings which become more and more similar to the regular lattice with increasing distance from the core.

Therefore, one may imagine a rather sharp distribution of levels of impurities accommodated in the core region, differing strongly from that of the same species located in the regular lattice. In contrast, the point defects located in the cloud formed by the strain field may generate a broader distribution of levels. Inside the cloud, point defects close to the core region are more strongly affected than the impurities located in the tail of the strain field. The latter are expected to form levels similar to isolated impurities in the regular lattice. Hence, the broad distribution of levels formed in the cloud may range between core-mediated impurity levels and levels similar to isolated impurities.

If the number of point defects/impurity atoms is small enough there is a high probability that they are accommodated mainly in the dislocation core. In that case, one expects a rather sharp distribution of levels as observed for dislocations with type 2 behaviour (a few 10^4 levels per cm). When the

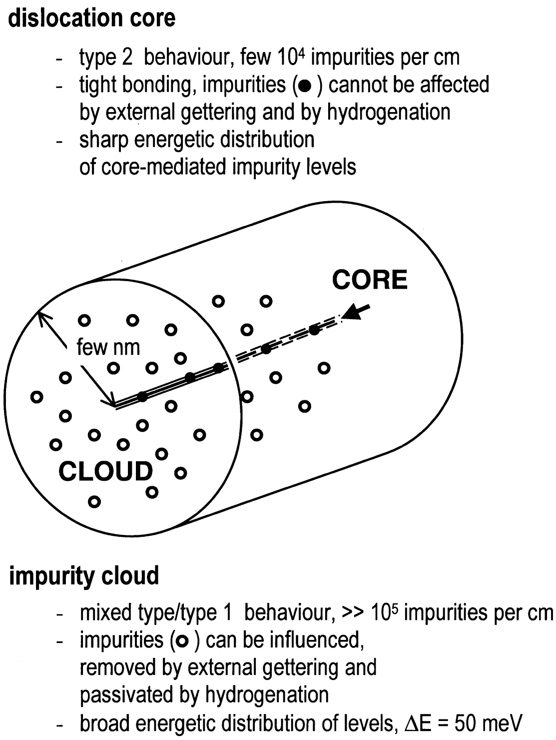

Fig. 5. Suggested behaviour of impurities accommodated at a dislocation (schematic). Note that a cloud of impurities is formed in the dilatation field of the dislocation. For simplicity we show here a circular distribution around the dislocation. Impurity atoms in the dislocation core are tightly bonded and cannot be affected by external gettering and hydrogenation, while those atoms accommodated in the cloud surrounding the dislocation can be removed by external gettering and passivated by hydrogen.

degree of contamination increases a large fraction of point defects may be located in the cloud formed by the strain field, extending a few nm from the core. Consequently, one may expect a broad distribution of levels, as in fact observed for dislocations of mixed type/type 1 behaviour (a few 10^5 levels per cm).

5. Limit of action of passivation and external gettering

The picture outlined may also be helpful to explain the observed limits of gettering and passivation treatments. EBIC investigations have shown that a deep-level density of 10^4–10^5 per cm dislocation length remains active after passivation and gettering [8,9]. Using the above arguments we can understand this experimental observation as follows (see also Fig. 5). (i) Impurities accommodated in the cloud surrounding the dislocation are weakly bound and can be passivated by hydrogen and/or can be removed by (phosphorus diffusion) gettering. (ii) In contrast, impurities accommodated in the dislocation core are strongly bound. We believe that this is why the core-mediated impurity levels can neither be affected by hydrogenation nor removed by external gettering sinks.

Indeed, from our DLTS observations we concluded that only a few 10^4 impurities per cm dislocation length are accommodated in the dislocation core, and that the impurity atoms will be accommodated in the dislocation cloud for higher densities of contamination. It should be pointed out that simulation and further experimental work will be needed to prove the above suggestions.

References

[1] D.K. Schroder, Solid State Phenom. 6/7 (1989) 383.
[2] M. Kittler, W. Seifert, Phys. Status Solidi (a) 99 (1987) 559.
[3] C. Donolato, M. Kittler, J. Appl. Phys. 63 (1988) 1569.
[4] M. Kittler, W. Seifert, Phys. Status Solidi (a) 138 (1993) 687.
[5] M. Kittler, C. Ulhaq-Bouillet, V. Higgs, J. Appl. Phys. 78 (1995) 4573.
[6] W. Seifert, M. Kittler, J. Vanhellemont, E. Simoen, C. Claeys, F.G. Kirscht, Inst. Phys. Conf. Ser. 149 (1996) 319.
[7] M. Kittler, W. Seifert, Phys. Status Solidi (a) 150 (1995) 463.
[8] K. Knobloch, M. Kittler, W. Seifert, J.J. Simon, I. Perichaud, Solid State Phenom. 63/64 (1998) 509.
[9] M. Kittler, C. Ulhaq-Bouillet, V. Higgs, Mater. Sci. Forum 196–201 (1995) 383.
[10] V. Kveder, M. Kittler, W. Schröter, Phys. Rev. B 63 (2001) 115208.
[11] K. Knobloch, M. Kittler, W. Seifert, Influence of contamination on the dislocation-related C1 line observed in DLTS spectra of n-type Si: a comparison with EBIC (accepted for publication in J. Appl. Phys.).
[12] P. Omling, E.R. Weber, L. Montelius, H. Alexander, J. Michel, Phys. Rev. B 32 (1985) 6571.
[13] D. Cavalcoli, A. Cavallini, E. Gombia, Phys. Rev. B 56 (1997) 10208.
[14] M. Kittler, W. Seifert, V. Kveder, in: B.L. Sopori (Ed.), Proceedings of the 11th Workshop on Crystalline Silicon Solar Cell Materials and Processes, Estes Park, CO, USA, August 19–22, 2001, pp. 32–39, NREL/BK-520-30.
[15] J. Kronewitz, W. Schröter, Izv. Akad. Nauk SSSR, Ser. Fiz. 51 (1987) 682.
[16] W. Schröter, H. Cerva, Interaction of Point Defects with Dislocations in Silicon and Germanium: Electrical and Optical Effects, in: S. Pizzini (Ed.), Defect Interaction and Clustering, Solid State Phenomena, Vols. 85/86 (2002) 67